full-scale flight tests of the B-747 airplane, it is expected that the use of flight spoilers on both the DC-10-30 and L-1011 airplanes also would be effective in attenuating the trailing vortex behind both of these airplanes.

Concluding Remarks

Based on the results obtained in these investigations, it was found by ground-based tests and verified by full-scale flight tests that the existing flight spoilers on the B-747 airplane are effective as trailing vortex attenuators. Based on the results of wind-tunnel investigations of the DC-10-30 and L-1011 airplane models, the existing flight spoilers on both the DC-10-30 and L-1011 airplanes are also expected to be effective trailing vortex attenuators.

References

[1] Croom, D. R., "Low-Speed Wind-Tunnel Investigation of Various Segments of Flight Spoilers as Trailing-Vortex-Alleviation Devices on a Transport Aircraft Model," NASA TN D-8162, 1976.

[2] Croom, D. R., Vogler, R. D., and Thelander, J. A., "Low-Speed Wing-Tunnel Investigation of Flight Spoilers as Trailing-Vortex-Alleviation Devices on an Extended Range Wide-Body Tri-Jet Airplane Model," NASA TN D-8373, 1976.

[3] Croom, D. R., Vogler, R. D., and Williams, G. M., "Low-Speed Wind-Tunnel Investigation of Flight Spoilers as Trailing-Vortex-Alleviation Devices on a Medium-Range Wide-Body Tri-Jet Airplane Model," NASA TN D-8360, 1976.

[4] Barber, M. R., Hastings, E. C. Jr., Champine, R. A. and Tymczyszyn, J. J., "Vortex Attenuation Flight Experiment," NASA SP-409, Wake Vortex Minimization, 1976.

Consideration of Clogging in Boundary-Layer Control System Design

Peter Crimi*
Avco Systems Division, Wilmington, Mass.

Introduction

BOUNDARY-LAYER control systems that employ suction through perforated or porous surfaces are subject to clogging by airborne sand and dust particles. Critics of boundary-layer control have often cited this problem as a serious limitation to practical application of boundary-layer control.[1] An analysis was undertaken to define the principal parameters affecting the clogging problem and to determine whether clogging could be alleviated or eliminated through proper design. A model for the clogging mechanism has been developed, the primary parameters of which are perforation size, particle size, boundary-layer thickness and velocity profile, external flow static and dynamic pressures, and suction pressure. Two different applications of boundary-layer control were analyzed, and design limitations to avoid clogging of systems used to prevent leading-edge stall have been delineated. Consideration has been directed specifically to systems employing perforations. The results obtained should also be applicable, however, at least qualitatively, to systems using porous surfaces made, for example, from sintered metals.

Received Feb. 23, 1977; revision received April 20, 1977.

Index categories: Subsystem Design; Boundary Layers and Convective Heat Transfer – Laminar; Boundary Layers and Convective Heat Transfer – Turbulent.

*Senior Consulting Scientist.

Model for Clogging

Consider, as an analogue of the physical problem, a spherical particle of diameter D_p lodged in a circular hole of diameter D_h, as sketched in Fig. 1. The particle is subjected to a shear flow, either laminar or turbulent, in which the magnitude of the fluid velocity is denoted $U(y)$. The portion of the sphere inside the hole is subjected to suction pressure p_s, which is necessarily less than the pressure p_e of the external flow.

The lift on the particle is assumed to be negligible in comparison to the force due to suction pressure. To evaluate the drag on the particle, it is first assumed that the drag coefficient C_D of the exposed portion, for a uniform freestream, is the same as that of a complete sphere. This is a reasonable assumption, since a hemisphere and a sphere have very nearly the same drag coefficient, provided projected area normal to the flow is used as reference area. It is further assumed that the drag per unit height on a horizontal section of the particle, denoted $d(y)$, is a weighted fraction of the total drag, using the product of U^2 and local width $b(y)$ as weighting function. Thus

$$d(y) = C_D \frac{\rho}{2} U^2(y) b(y) \tag{1}$$

This strip, or slab, formulation is similar to the method used to evaluate drag on buildings subjected to wind shear, whereby the mean value, over the height of the building, of the dynamic pressure is substituted in the expression for the drag.[2]

The limiting condition for no clogging of an individual particle is achieved when the moment due to drag about the furthest downstream contact point is just sufficient to overcome the moment due to the suction on the portion of the particle in the hole. This condition is expressed analytically by

$$\frac{(p_e - p_s)_{\max}}{q_e} = \frac{16 C_D}{\pi D_h^3} \int_0^h y b(y) \left(\frac{U}{U_e}\right)^2 dy \tag{2}$$

where U_e and p_e are the velocity and pressure in the external flow, respectively, and

$$q_e = \tfrac{1}{2}\rho U_e^2$$

$$h = \tfrac{1}{2}\left[D_p + \sqrt{D_p^2 - D_h^2}\right]$$

$$b = 2\sqrt{\left(\frac{D_p}{2}\right)^2 - \left(y - h + \frac{D_p}{2}\right)^2}$$

and ρ is the air density. Actual boundary-layer velocity profiles, either measured or calculated, could presumably be used in Eq. (2) to obtain the limiting condition. For present purposes, though, it was felt that the following approximations, taken from Ref. 3, would suffice:

Laminar	Turbulent
$\frac{U}{U_e} = \frac{2y}{\delta} - 2\left(\frac{y}{\delta}\right)^3 + \left(\frac{y}{\delta}\right)^4$	$\frac{U}{U_e} = \left(\frac{y}{\delta}\right)^{1/7}$ $y < \delta$
$\frac{U}{U_e} = 1$	$\frac{U}{U_e} = 1$ $y \geq \delta$
$\delta^*/\delta = 0.3$	$\delta^*/\delta = 0.125$

where δ^* is displacement thickness. A value of 0.4 was assigned to C_D for all calculations.

Applications to Specific Systems

Suction Limit for No Clogging

Two parameters define the limiting suction value prescribed by Eq. (2), namely, D_p/D_h and D_h/δ^*. For a given value of

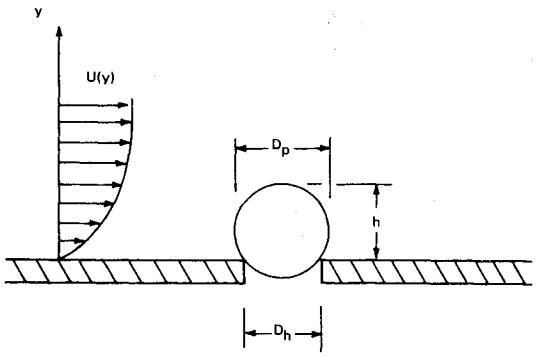

Fig. 1 Geometry for a lodged particle.

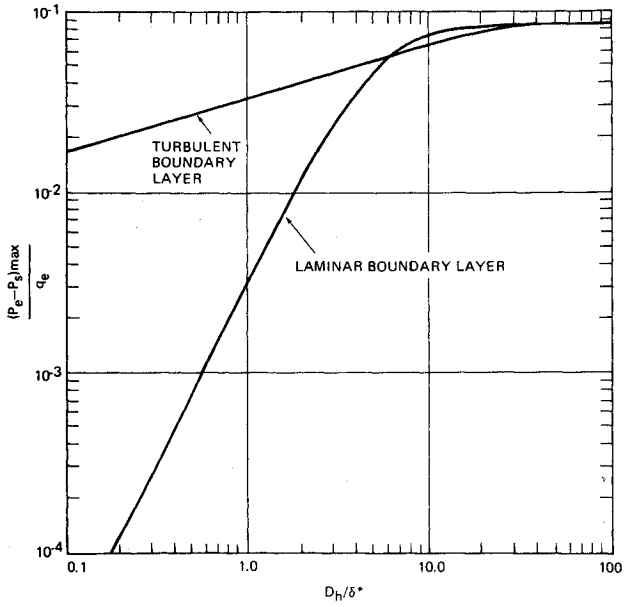

Fig. 2 Maximum pressure difference for no clogging vs hole size.

the latter ratio, the minimum of $(p_e - p_s)_{max}/q_e$ is obtained for $D_p/D_h = 1$. Thus, curves of maximum suction for no clogging vs hole size were obtained from Eq. (2) for both laminar and turbulent boundary layers by specifying that $D_p = D_h$ and evaluating the required integral numerically. The results are shown in Fig. 2. It is seen that, regardless of hole size, if $(p_e - p_s)/q_e$ exceeds 0.085, the system will be subject to clogging. Also, the value of the pressure limit is relatively insensitive to hole size for turbulent boundary layers, but decreases rapidly with decreasing hole size for laminar boundary layers when D_h is less than about $4\delta^*$.

Result for System Using Area Suction

The U.S. Army XV-11A STOL airplane employed suction through perforations over most of the upper wing surface to prevent separation of the turbulent boundary layer and thereby achieve very high lift coefficients at low speed. As reported in Ref. 4, the system was designed to have a pressure difference across the suction surface of 9 in. of water. From Ref. 4, the pressure coefficient near midchord at a section lift coefficient of 2.01 was measured to be -2.3, which gives, for a forward speed of 50 mph, a value for U_e of 133 fps. Thus, for these conditions, it is found that $(p_e - p_s)/q_e = 2.2$, which grossly exceeds the calculated upper limit for no clogging of 0.085. It was further estimated from the data of Ref. 5 that $D_h/\delta^* = 0.694$ near midchord. It then follows, with the aid of Eq. (2), that particles with diameters in the range from 1-2.3 hole diameters (0.025-0.058 in.) will be trapped in the perforations when the system is operated at the design suction rate. It would appear, then, that systems of this type, requiring relatively high suction rates over a large area, generally will be subject to clogging.

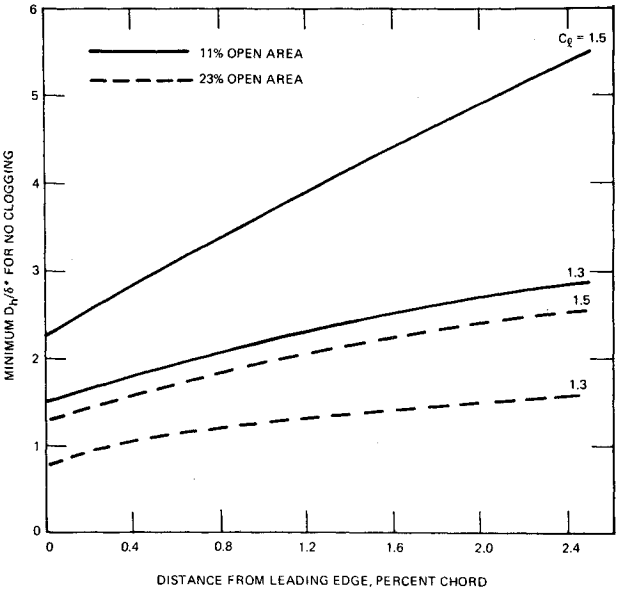

Fig. 3 Minimum hole size for no clogging vs distance from the leading edge for system used to prevent leading-edge stall.

Application to Systems Used for Control of Leading-Edge Stall

Leading-edge stall of airfoils can be prevented by suction at a relatively low rate over a small segment of the upper surface near the leading edge.[6] Susceptibility to clogging of this type of system was assessed for two sets of conditions using the data of Ref. 6, which reports tests of an NACA 63A009 airfoil section with suction applied from the leading edge to 2.75% of chord from the leading edge, on the upper surface only. Assuming a chordal Reynolds number of 4×10^6, the data of Ref. 6 give that a maximum lift coefficient of 1.3 is obtained with a mean suction velocity through the surface, v_0, of 0.030 times the freestream speed U_∞, and $C_{l_{max}} = 1.5$ with a v_0 of .050 U_∞. The suction velocity can be related directly to the pressure drop across the surface. From the data of Ref. 7, it is seen that the pressure drop for perforated surfaces is a function of the percent of open area and v_0, and is essentially independent of hole size. Furthermore, for a given percent open area, $p_e - p_s$ is, as a good approximation, proportional to $\frac{1}{2}\rho v_0^2$. For example, with 11% open area, it is found from Fig. 2 of Ref. 7 that $p_e - p_s \approx 126\,(\rho v_0^2/2)$ and with 23% open area, $p_e - p_s \approx 44(\rho v_0^2/2)$, for v_0 in the range from 10 to 60 fps. To compute $(p_e - p_s)/q_e$ for a specified C_l and v_0, the method of Ref. 8 was employed to obtain U_e/U_∞ as a function of distance from the leading edge, from which the surface variation of v_0/U_e, and hence $(p_e - p_s)/q_e$, was determined. For example, with $C_l = 1.3$, the procedures of Ref. 8 give that $U_e/U_\infty = 4.08$ at the leading edge so, for the case at hand, $v_0/U_e = 0.03/4.08 = 0.00735$, and $(p_e - p_s)/q_e = (126)(0.00735)^2 = 0.00681$ with 11% open area. From Fig. 2, then, the minimum hole diameter for no clogging at the leading edge is $1.52\delta^*$. This procedure was used to generate plots of minimum D_h/δ^* vs distance from the leading edge, which are given in Fig. 3. These minimums are not likely to conflict with any structural requirements for hole size, but some difficulty with uniformity of the flow in the boundary layer might be encountered at the higher lift coefficient with 11% open area, as the minimum hole diameter is nearly two boundary-layer thicknesses ($7\delta^*$) at the downstream end of the suction surface. In general, however, it appears that clogging need not be a problem for boundary-layer control used to prevent leading-edge stall.

References

[1] Cornish, J. J., "Some Aerodynamic and Operational Problems of STOL Aircraft With Boundary-Layer Control," *Journal of Aircraft*, Vol. 2, March-April 1965, pp. 78-86.

[2] Hoerner, S., *Fluid-Dynamic Drag*, published by author, Midland Park, N. J., 1958.

[3] Schlichting, H., *Boundary Layer Theory*, McGraw-Hill, New York, 1960.

[4] Roberts, S. C. et. al., "XV-11A Description and Preliminary Flight Test," USAAVLABS Tech. Rept. 67-21, May 1967.

[5] Roberts, S. C., "The Marvel Report, Part E – Solution to the Problem of Obtaining Two-Dimensional Boundary Layer Data on the Variable-Camber High-Lift Wings of the Marvelette," U.S. Army TRECOM Tech. Rept. 65-16, May 1965.

[6] Gregory, N. and Walker, W. S., "Wind-Tunnel Tests on the NACA 63A009 Aerofoil with Distributed Suction Over the Nose," ARC R&M No. 2900, Sept. 1952.

[7] Dannenburg, R., Gambucci, B., and Weiberg, J., "Perforated Sheets as a Porous Material for Distributed Suction and Injection," NACA TN 3669, April 1956.

[8] Abbott, I. and Doenhoff, A., *Theory of Wing Sections*, Dover, New York, 1959.

Dynamic Blade Row Compression Component Model for Stability Studies

W.A. Tesch* and W.G. Steenken†

General Electric Company, Cincinnati, Ohio

Nomenclature

A = area
$A_{1\beta}$ = area normal to relative flow
C = axial velocity
C_T = absolute tangential velocity
IGV = inlet guide vane
L = volume length
M = Mach number
N = wheel speed
P = static pressure
P_d = dynamic pressure ($P_T - P$)
P_T = total pressure
S = entropy
V = volume
W = physical flow rate
a = acoustic velocity
q = kinetic pressure ($\frac{1}{2}\rho v^2$)
r = pitch-line radius
v = velocity
t = time

Introduction

PREDICTING the stability characteristics of turbofan engines when subjected to a wide variety of steady and unsteady inlet flow distortions remains a continuing problem that must be solved successfully if airframe/engine integration is to occur with no inlet/engine compatibility problems. To date, the engine developer has relied upon historical data and empirical correlations. However, such approaches, although providing visibility at the inlet/engine interface, do not lend themselves to understanding the impact of compressor design variables when trying to achieve a solution to potential or existing stability problems.

As a first step in developing a compression system stability analysis tool, an operationally verified compression component stability model has been developed, which accurately reproduces experimentally determined speed lines and accurately predicts the associated surge point. The following discussion which is taken from Ref. 1 describes this model, the manner in which a solution is achieved, and the results obtained by simulating an eight-stage compressor.

Formulation of Model

This analysis begins with the complete set of nonlinear partial differential equations known as the equations of change[2] which describe the transport processes within a fluid. These equations have been integrated once over an arbitrary control volume of the flow system to obtain the "macroscopic balances." It should be noted that the energy equation was combined with one of the thermodynamic *Tds* relationships[3] prior to integration. The "macroscopic balances" for mass, momentum, and energy, respectively, are reproduced here in the form that they are used in the dynamic model:

$$\frac{\partial \bar{\rho}}{\partial t} = \frac{1}{V}(W_1 - W_2) \tag{1}$$

$$\frac{\partial \bar{W}}{\partial t} = \frac{1}{L}[W_1 C_1 - W_2 C_2 + P_1 A_1 - P_2 A_2 - P_M (A_1 - A_2) + F_B] \tag{2}$$

$$\frac{\partial \overline{\rho S}}{\partial t} = \frac{1}{V}[W_1 S_1 - W_2 S_2 + S_F] \tag{3}$$

The variables subscripted by 1 and 2 on the right-hand side of the equations refer to quantities at the inlet and exit stations of the control volume, respectively. The left-hand side of the equation represents time derivatives of volume averaged properties. With reference to Fig. 1, it is seen that P_M represents the mean pressure acting on the lateral area of the fluid, and F_B is the blade force acting upon the fluid. The term S_F, the total rate of irreversible conversion of mechanical to internal energy, in the case of this model represents the entropy production caused by blade row losses.

Equations (1-3), other than being applicable to quasi-one-dimensional flows in finite volumes without heat transfer, properly describe the state of a fluid in motion. In order for a solution to be obtained, it is necessary to supply the caloric and thermal equations of state and expressions for P_M, S_F, and F_B.

The mean pressure term represents the mean of the static pressure distribution acting on the lateral surface of the blade row and free volumes. The complication introduced by this term results from the fact that rigorous determination of its value requires invoking the momentum equation and can lead to over constraint of the system of equations. The mean pressure for blade row volumes is determined from the empirical relationship where

$$P_M = (2P_L + P_S)/3 \tag{4}$$

P_L is the larger of the volume inlet or exit station static pressures, and P_S is the smaller of the volume inlet or exit station static pressures. This empirical relationship was developed by examining an exact calculation of the mean pressure in a compression component with no losses and assuming that the relationship developed for lossless blade rows would remain valid for the actual case where blade row losses are taken into account. The mean pressure for free

Presented as Paper 76-203 at the AIAA 14th Aerospace Sciences Meeting, Washington, D. C., Jan. 26-28, 1976; submitted March 23, 1976; revision received April 29, 1977.

Index categories: Airbreathing Propulsion; Nonsteady Aerodynamics; Computational Methods.

*Engineer, Stability and Installation Aerodynamics, Aircraft Engine Group.

†Manager, Stability and Installation Aerodynamics, Aircraft Engine Group. Associate Fellow AIAA.